PROCEEDINGS OF SCIENCE

The Greisen function and its ability to describe air shower profiles

Maximilian Stadelmaier,[a,*] **Vladimír Novotný**[a,b] **and Jakub Vícha**[a]

[a] *Institute of Physics of the Czech Academy of Sciences, Prague, Czech Republic*

[b] *Institute of Particle and Nuclear Physics, Faculty of Mathematics and Physics, Charles University, Prague, Czech Republic*

E-mail: stadelmaier@fzu.cz

Extensive air showers are one of the most important phenomena to study in the context of ultrahigh-energy cosmic rays. Their longitudinal development can be directly observed using fluorescence detector telescopes, such as those employed at the Pierre Auger Observatory or the Telescope Array. In this work, we discuss the properties of the Greisen function, originally introduced to describe the longitudinal shower profiles of electromagnetic air showers, and demonstrate that, after appropriate modification, it can be used to describe longitudinal air-shower profiles, even for hadronic air showers. Furthermore we discuss the possibility to discriminate between hadrons and photons from the shape of air-shower profiles using the Greisen function.

38th International Cosmic Ray Conference (ICRC2023)
26 July - 3 August, 2023
Nagoya, Japan

*Speaker

https://pos.sissa.it/

PoS(ICRC2023)340

1. Introduction

High-energy cosmic rays create cascades of secondary particles upon interaction with the Earth's atmosphere, which are known as extensive air showers [1, 2]. Particles created in extensive air showers can be detected at the ground using surface detector arrays, but can also be observed using fluorescence detector telescopes from the light they produce by excitation of nitrogen molecules in the atmosphere. The characteristic curve of the development of emitted fluorescence light as a function of the surpassed calorimetric matter, which directly follows the energy deposit in the atmosphere, is known as the longitudinal shower profile. To reconstruct the shower profile and related observables, a profile function needs to be fitted to the detector data. Gaisser and Hillas proposed an empiric function [3] to describe the longitudinal development of proton air showers in the context of the Constant Intensity Cut method [4, 5], which is used in surface detector experiments to take into account the atmospheric attenuation of particles in air showers from different zenith angles. Today, both the Pierre Auger Observatory and the Telescope Array use the Gaisser-Hillas function to describe shower profiles from their fluorescence detector data [6, 7].

In this work, we present the Greisen function and its properties. We review the origin of the function itself and introduce minor modifications to the Greisen function to make it a handy function to fit shower profile data. We will demonstrate the usability of the Greisen function as an alternative to the Gaisser-Hillas function to describe shower profiles and present its performance to reconstruct the depth $X_{\max}$ of the shower maximum as well as the primary energy using Monte Carlo (MC) simulations of air showers.

2. The Greisen Function

More than 80 years ago, Rossi and Greisen derived functions to describe the average longitudinal development of electromagnetic air showers [8]. This description holds in good approximation also for hadronic showers, initiated by protons and heavier nuclei, which seem to make up the upper end of the cosmic-ray energy spectrum [9]. Their solutions to the differential equations that describe electromagnetic cascades were used to motivate important properties in the context of air-shower physics, such as the shower age. The shower age parameter s describes an electromagnetic shower, initiated by a primary particle of the energy E_0, after t radiation lengths, considering only the particles above an energy of E_{cut}. It is given as

$$s = \frac{3t}{t + 2\beta}, \tag{1}$$

with $\beta = \ln(E_0/E_{\mathrm{cut}})$; the spectra of the electromagnetic particles in a shower approximately follow a power-law distribution of the form $\sim E^{-(s+1)}$. In general, $s = 0$ at the beginning of the shower cascade, $s = 1$ at its maximum, and $s \gg 1$ once most particles have been attenuated. For electromagnetic showers a reasonable choice for E_{cut} is close to 87 MeV, which is the energy above which electromagnetic particles on average lose more energy in radiative shower processes than to scattering and ionization. To describe the number of particles N above ≈100 MeV as a function of t, the Greisen function was introduced in [10] and reads as

$$N(t) = \frac{0.31}{\sqrt{\beta}} \exp\left[t\left(1 - \tfrac{3}{2}\ln s\right)\right]. \tag{2}$$

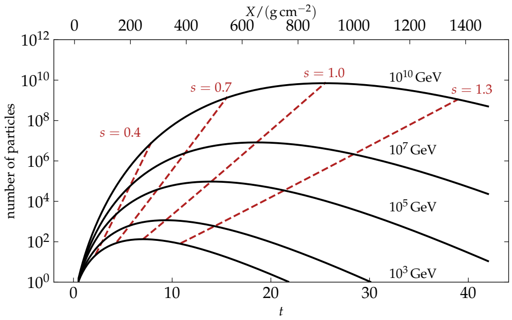

Figure 1: Sketch of the Greisen function evaluated for different primary energies. The top axis converts t to atmospheric depth using $X/t = 37\,\mathrm{g\,cm^{-2}}$. Red dashed lines represent regions of equal shower age s for different primary energies.

A depiction of the behavior of the Greisen function is given in Fig. 1. A derivation of Eq. (2) is given in [11].

To be able to use the Greisen function to describe shower profile data, we have to overcome two major shortcomings of the function as written in Eq. (2). Firstly, the Greisen function in its classic form cannot account for different points of the first interaction of the cascade, since by construction the shower is initiated at $t = 0$. Secondly, the scale of the Greisen function is only accurate for the number of particles above $\approx$100 MeV in the average electromagnetic shower. We insert the point of the first interaction as a free parameter, and we introduce a new parameter ϵ. We demonstrate that the Greisen function generalized this way is able to describe the longitudinal profile of individual electromagnetic and hadronic showers as well as the corresponding shower-to-shower fluctuations.

3. The Modified Greisen Function

We propose two intuitive modifications to the classical Greisen function, given in Eq. (2), to make it able to describe the energy deposit as a function of the atmospheric depth of individual electromagnetic and hadronic showers of cosmic rays at ultra-high energies. Firstly, we introduce a non-zero point of the first interaction at a slanted atmospheric depth X_1, that will be described by $t_1 = X_1/X_0$ using the radiation length[1] X_0. Equivalently, we use $t = X/X_0$ and $t_{\max} = X_{\max}/X_0$. Thus, the shower age s will be given as

$$s = \frac{3t'}{t' + 2\beta}\,\Theta(t'), \tag{3}$$

with $t' = t - t_1$, using the Heaviside function Θ. To maintain the property of the shower age, which is supposed to be 1 at the maximum of the shower, and to keep number of radiation lengths required to reach the maximum of the shower the same as before, we redefine β in accordance with the previous modification as

$$\beta = \ln(E_0/E_{\mathrm{cut}}) = t_{\max} - t_1. \tag{4}$$

Finally, to replace the constant 0.31 in Eq. (2), we introduce the factor ϵ, which is defined in units of energy deposit per step length, and which can be interpreted as effective energy loss per particle and step length at the shower maximum. Thus, the modified Greisen profile reads as

[1]For electromagnetic showers X_0 corresponds to the electromagnetic radiation length in air of $\approx 37\,\mathrm{g\,cm^{-2}}$, for hadronic showers X_0 takes an effective value larger than the electromagnetic radiation length.

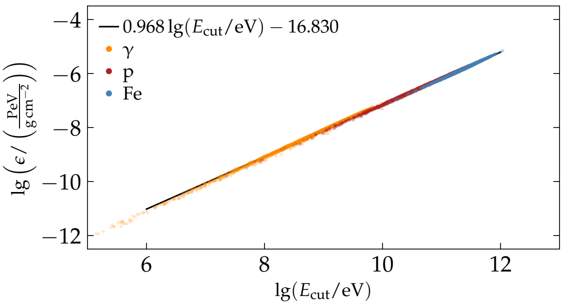

Figure 2: Correlation of ϵ and E_{cut} for simulated air showers [11].

$$\frac{\mathrm{d}E}{\mathrm{d}X}(t) \equiv N(t) = \frac{\epsilon}{\sqrt{\beta}} \exp\left[(t - t_1)\left(1 - \tfrac{3}{2}\ln s\right)\right], \tag{5}$$

with $N(t) = 0$ for $t \leq t_1$. For the sake of simplicity, here and in the following, in the text we abbreviate the energy deposit $\mathrm{d}E/\mathrm{d}X$ with the symbol N, which was reserved for the number of particles in Section 2.

4. Describing Shower-to-Shower Fluctuations and the Shape of the Profile

If Eq. (5) is used to describe shower profiles, one can calculate event-level values for ϵ and E_{cut} from the MC values of X_{max}, X_1, $N(t_{max})$, and E_0. From Eqs. (4) and (5) it is readily found that

$$\epsilon = N(t_{max})\sqrt{\beta}\,\mathrm{e}^{-\beta} \tag{6}$$

and

$$E_{cut} = E_0\,\mathrm{e}^{-\beta}. \tag{7}$$

To calculate β for the MC shower profiles we use $X_0 = 40\,\mathrm{g\,cm^{-2}}$ as a reasonable compromise for hadronic and electromagnetic showers. Note that because of the implicit dependence of both β and the average $N(t_{max})$ on the primary energy, the dependence of ϵ as well as of E_{cut} on E_0 cancels. In Fig. 2 we present the correlation observed between ϵ and E_{cut} when examining showers from photons, protons, and iron nuclei, at primary energies of $10^{18.5}$ eV, $10^{19.0}$ eV, and $10^{19.5}$ eV, simulated with the Sibyll2.3d [12] model of hadronic interactions. The simulations were produced using the Conex [13] event generator at version v7.60. The examined simulation library contains 1000 showers for each combination of primary particle and energy. We find an almost perfect correlation of ϵ with the effective threshold energy E_{cut} (see Eq. (4)). Thus we expect mass composition sensitive behavior of ϵ. In the following, we will discuss how ϵ is related to the shape and the type of the primary particle of individual shower profiles.

The dependence of the shape of the shower profiles on the type of the primary particles becomes more obvious when the dependence on the primary energy and the shower-to-shower fluctuations (i.e. differences in the profiles from showers, which were induced by the same primary at the same energy) are partially removed. Integrating the Greisen function as given in Eq. (5) yields the

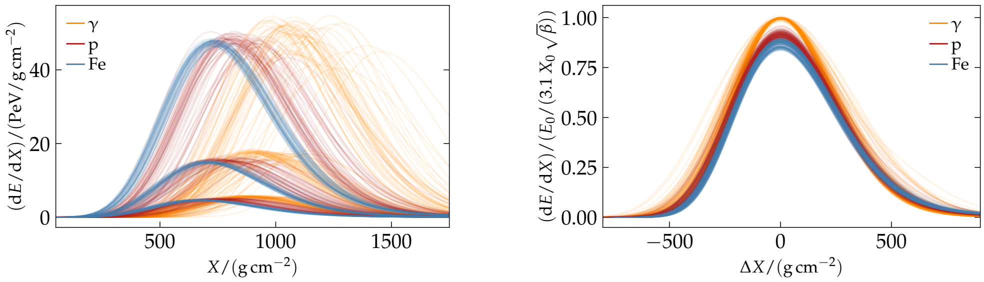

Figure 3: Left: Simulated shower profiles with primary energies of $10^{18.5}$, eV, 10^{19} eV, and $10^{19.5}$ eV using different primary particles. Shower-to-shower fluctuations are visible in addition to the increase of the profile size depending on the primary energy. **Right:** The same profiles scaled and shifted; see the text for details.

calorimetric energy deposit of a shower profile, which for purely electromagnetic showers is very close to the primary energy, E_0. Numerically, we find that

$$\int_{X_1}^{\infty} \frac{\epsilon}{\sqrt{\beta}} \exp\left[(X - X_1)/(X_0)\left(1 - \tfrac{3}{2}\ln s\right)\right] \mathrm{d}X \simeq 3.1\,\epsilon\,\mathrm{e}^{\beta}\,X_0 \tag{8}$$

is a good approximation for the integrated Greisen profile. Thus, normalizing the shower profile using Eqs. (6) and (8) and shifting the ordinate of the profiles to use the shower maxima as a common point of reference, $\Delta X = X - X_{\max}$, we can highlight subtle differences in the shower profiles for the different primary particles, as can be seen in Fig. 3. On average, we expect a longer "*tail*" for hadronic showers, as well as smaller values for $X_{\max} - X_1$. Furthermore, the size of the maximum of the Greisen function, $N(t_{\max}) = \epsilon\,\mathrm{e}^{\beta}/\sqrt{\beta}$, is mainly governed by the factor e^{β}, which depends on X_1, X_0, and $X_{\max}$. Hence ϵ, as a pre-factor, will compensate subtle changes in the shape. However, as can be seen in Fig. 3 (*right*), the differences in the shape of the profiles for different primary particles are subtle, consequently the mass composition sensitivity of ϵ will diminish for data from low-energy showers that is subject to a lot of noise.

The behavior displayed in Figs. 2 and 3 using the Sibyll2.3d model of hadronic interactions is also apparent for simulations using the Epos-lhc [14] or the QgsjetII-04 [15] model of hadronic interactions. We find that shower-to-shower fluctuations, that manifest not only in different values of $X_{\max}$, but also in differences in the shape of the profile, can be described by the modified Greisen function.

The mass-composition sensitivity of the shape of shower profiles has been investigated already using the Gaisser-Hillas function [16], especially in the context of a reparametrized version of the Gaisser-Hillas function using "L" and "R". The Greisen function, however, yields a promising alternative because the shape can be elegantly described using only the parameter ϵ.

5. Fitting the Greisen Function to Simulated Data

To extract information about air shower profiles from detector data, a profile function needs to be fitted to the reconstructed energy deposit as a function of the atmospheric depth. Most commonly

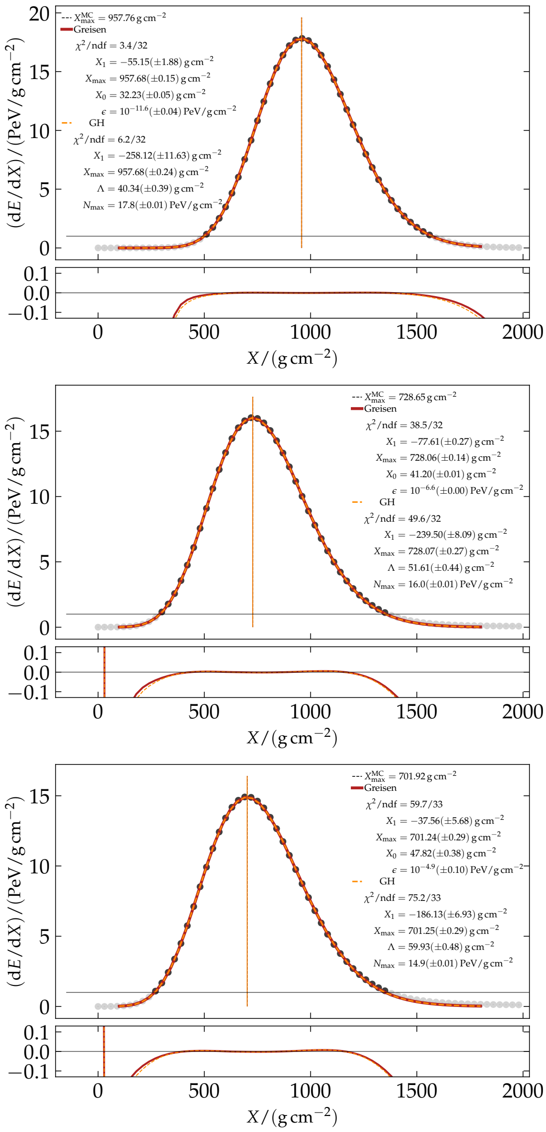

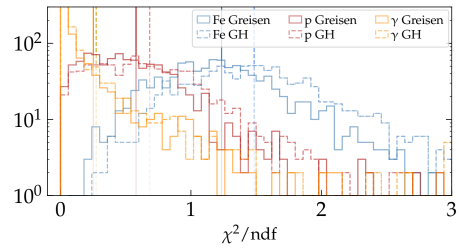

Figure 4: Left: Simulated example profiles from (*top to bottom*) photon, proton, and iron nucleus as primary particles. Both the Greisen function (red) and the Gaisser-Hillas function (orange, dashed) are fitted to the profile data. The legend of each panel displays the MC values of $X_{\max}$ as well as the best-fit parameters of the two functions f to describe the shower profile data d. The lower panel depicts the relative difference $\delta = (f - d)/d$ of the profile functions with respect to the data. The "tails" of the profiles, which were disregarded for the fit, are indicated as gray markers. **Right:** Distributions of χ^2/ndf for the Greisen function and Gaisser-Hillas function fitted to simulated shower profiles with a primary energy of 10^{19} eV for different primary particles. The means of the distributions are indicated by a vertical line.

this is done using the Gaisser-Hillas function [3],

$$\frac{\mathrm{d}E}{\mathrm{d}X} = N_{\max} \left(\frac{X - X_1}{X_{\max} - X_1} \right)^{\frac{X_{\max} - X_1}{\Lambda}} \exp\left[\frac{X_{\max} - X}{\Lambda} \right], \tag{9}$$

but also different functions (e.g. a Gaussian) have been tested for this purpose in the past [17]. In the following, we fit the Greisen function alongside the Gaisser-Hillas function to simulated ideal shower profiles. The uncertainty for the individual data points was set at a constant value so that a mix of shower profiles from protons and iron nuclei will result in $\chi^2/\mathrm{ndf} \simeq 1$ at a primary energy of 10^{19} eV for reference. Example fits of the two functions to simulated shower profiles with a primary energy of 10^{19} eV are depicted in Fig. 4 alongside distributions of χ^2/ndf. From visual inspection there is little to no difference in the best fit realizations of the Greisen and the Gaisser-Hillas function using the same simulated data. However, the Greisen function yields a ≈10% improvement in the average χ^2/ndf for hadronic showers.

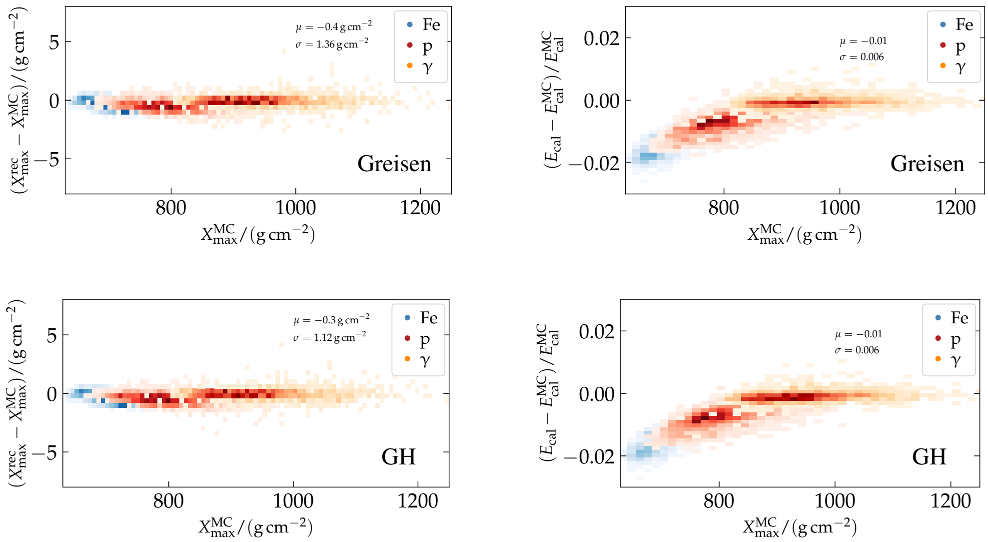

Figure 5: Top: Residuals of the MC and recovered values of X_{max} (*left*) and E_{cal} (*right*) using the Greisen function. **Bottom:** The same data obtained using the Gaisser-Hillas function.

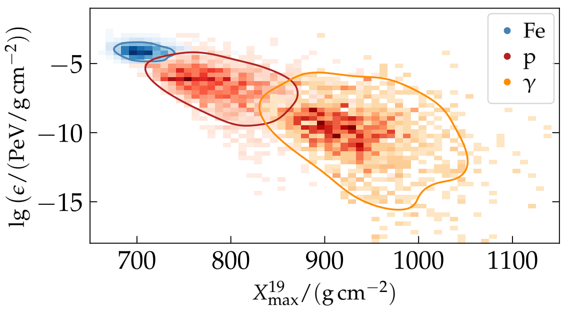

Figure 6: Distributions of ϵ and X_{max}^{19} as two-dimensional histograms.

The most interesting observables to extract from shower profile data are the depth of the maximum, X_{max}, and the calorimetric energy deposit[2], E_{cal}, from which the energy of the primary can be estimated. We extract both from the best fit values of the Greisen and the Gaisser-Hillas function fitted to the simulated shower profiles. The residuals of the recovered and true values are depicted in Fig. 5 as a function of the MC values of X_{max}. Both the Greisen and the Gaisser-Hillas function provide an accurate result for the depth of the shower maximum. Furthermore, we observe the same accuracy and precision when recovering E_{cal} for both fitted profile functions. There is a slight negative bias that increases with the amount of hadronization occurring in the shower and is at approximately -2% for showers induced by iron nuclei.

Whilst the Greisen function on average shows a slightly better value for χ^2/ndf for all primary particles, the performance to recover X_{max} and E_{cal} is identical to the Gaisser-Hillas function. Additionally, in Fig. 6 we present the mass-composition sensitive parameters from the best-fit values of the Greisen function parameters. As X_{max} on its own is not mass-composition sensitive

[2]We calculate the MC calorimetric energy deposit from the sum of the simulated profile data, and the reconstructed calorimetric energy from the profile function by numerical integration from $0\,\mathrm{g\,cm^{-2}}$ to $2000\,\mathrm{g\,cm^{-2}}$.

without knowledge about the primary energy [18], we subtract a constant decadal elongation rate and use $E_0 = 10^{19}$ eV as a reference, $X_{\max}^{19} = X_{\max} - 58\,\mathrm{g\,cm^{-2}}\,\lg(E_0/10^{19}\,\mathrm{eV})$. We observe only a mild correlation of ϵ and $X_{\max}^{19}$ for the individual primaries[3] and thus consider the behavior depicted in Fig. 6 not as artificial. Thus the mass-sensitivity of ϵ partially adds to the sensitivity of $X_{\max}$.

6. Summary and Conclusion

In this work we discuss the behavior of the well-known Greisen function, which was introduced to describe average electromagnetic air-shower profiles. We suggest minor intuitive modifications, with which the Greisen function is made able to describe individual showers from both electromagnetic and hadronic primary particles. Furthermore, we discuss the mass-composition sensitivity of the shape of shower profiles. We present the performance of the Greisen function to recover the depth of the shower maximum as well as the calorimetric energy deposit when fitted to ideal simulated shower profiles and find that it is not second to the classic Gaisser-Hillas function. Additionally, we introduce the parameter ϵ that carries information about the mass of primary particle, additionally to the depth of the shower maximum.

7. Acknowledgements

The authors would like to thank Alexey Yushkov, Eva Santos, and Darko Veberič for fruitful comments and discussions. This work was partially supported by the Ministry of Education Youth and Sports of the Czech Republic and by the European Union under the grant FZU researchers, technical and administrative staff mobility, registration number CZ.02.2.69/0.0/0.0/18_053/0016627. This work was supported by the Czech Science Foundation – Grant No. 21-02226M.

References

[1] B. Rossi, *Z. Phys.* **82** (1933) 151.
[2] P. Auger, P. Ehrenfest, R. Maze, J. Daudin and A.F. Robley, *Rev. Mod. Phys.* **11** (1939) 288.
[3] T.K. Gaisser and A.M. Hillas, *Proc. Int. Cosmic Ray Conf.* **8** (1977) 353.
[4] J. Hersil, I. Escobar, D. Scott, G. Clark and S. Olbert, *Phys. Rev. Lett.* **6** (1961) 22.
[5] J. Alvarez-Muniz, R. Engel, T.K. Gaisser, J.A. Ortiz and T. Stanev, *Phys. Rev. D* **66** (2002) 123004 [astro-ph/0209117].
[6] Pierre Auger Collaboration, *Phys. Rev. D* **90** (2014) 122005 [1409.4809].
[7] Telescope Array Collaboration, *Astrophys. J.* **858** (2018) 76 [1801.09784].
[8] B. Rossi and K. Greisen, *Rev. Mod. Phys.* **13** (1941) 240.
[9] K.-H. Kampert and M. Unger, *Astropart. Phys.* **35** (2012) 660 [1201.0018].
[10] K. Greisen, *Progress in Cosmic Ray Physics* **3** (1956) 3.
[11] M. Stadelmaier, J. Vícha and V. Novotný, *Phys. Rev. D* **107** (2023) 103056 [2303.16670].
[12] F. Riehn, R. Engel, A. Fedynitch, T.K. Gaisser and T. Stanev, *Phys. Rev. D* **102** (2020) 063002 [1912.03300].
[13] T. Bergmann, R. Engel, D. Heck, N.N. Kalmykov, S. Ostapchenko, T. Pierog et al., *Astropart. Phys.* **26** (2007) 420 [astro-ph/0606564].
[14] T. Pierog, I. Karpenko, J.M. Katzy, E. Yatsenko and K. Werner, *Phys. Rev. C* **92** (2015) 034906 [1306.0121].
[15] S. Ostapchenko, *Phys. Rev. D* **83** (2011) 014018 [1010.1869].
[16] S. Andringa, R. Conceicao and M. Pimenta, *Astropart. Phys.* **34** (2011) 360.
[17] R.M. Baltrusaitis et al., *Nucl. Instrum. Meth. A* **240** (1985) 410.
[18] J. Matthews, *Astropart. Phys.* **22** (2005) 387.

[3] The Pearson correlation, $\mathrm{cov}(X,Y)/\sqrt{\mathrm{var}(X)\,\mathrm{var}(Y)}$, using $X = X_{\max}^{19}$ and $Y = \lg(\epsilon/(\mathrm{PeV}/(\mathrm{g\,cm^{-2}})))$ is -0.32 for iron nuclei, and -0.45 for both protons and photons as primary particles.